3D VISUALIZATION AND IRRIGATION DECISION DESIGN FOR TEA GARDENS BASED ON DIGITAL TWIN

/

基于数字孪生的茶园三维可视化与喷灌决策设计

Xiuyan ZHAO[1)], Xiaomeng SHANG[1)], Dongge YUAN[2)], Zhaotang DING[3)], Zhenzhen XU[4)], Riheng WU[1)], Kaixing ZHANG[5)]

[1)] College of Information Science and Engineering, Shandong Agricultural University, Taian 271018, China

[2)] Weichai Lovol Smart Agriculture Technology Co., Ltd., Weifang 261000, China

[3)] Tea Research Institute, Shandong Academy of Agricultural Sciences, Jinan 250100, China

[4)] Shandong Panran Instrument Group Co., Ltd., Taian 271000, China

[5)] College of Mechanical and Electronic Engineering, Shandong Agricultural University, Taian 271018, China

Tel: 13954895451; E-mail: 13954895451@163.com

DOI: https://doi.org/10.35633/inmateh-77-35

Keywords: *Digital twin; AquaCrop-LSTM prediction model; Water demand forecasting; Decision management and control*

ABSTRACT

This study addresses the challenges of low-precision 3D visualization, unclear irrigation requirements, and inadequate smart decision-making in tea garden management. A twin data-driven 3D visualization and control system is proposed based on a six-dimensional digital twin framework, consisting of physical entities, virtual models, data connections, services, digital twin data, and decision mechanisms. First, real-time bidirectional data interaction is achieved through an OPC UA communication channel and multi-source sensor integration with a MySQL database. Second, parametric tea plant modeling in 3ds Max, combined with particle systems, dynamic shaders, ambient occlusion (AO), and level-of-detail (LOD) rendering, enables high-fidelity and dynamic 3D visualization. Finally, an AquaCrop-LSTM irrigation demand prediction model was developed by integrating the FAO Penman–Monteith method, the AquaCrop model, and a Long Short-Term Memory (LSTM) neural network. The complete system, deployed within Unity, forms a closed-loop architecture of perception, mapping, decision-making, and feedback. Experimental results show that the LOD strategy improves the frame rate by 121% while reducing vertex count by 93.7%. The AquaCrop-LSTM model achieves a mean absolute error (MAE) of 0.251 mm and an R^2 value of 0.927. Under a 30-user concurrent load test, the system maintained an error rate below 0.02%. These findings demonstrate that the proposed system provides reliable technical support for visual monitoring and efficient irrigation management in tea gardens.

摘要

针对茶园三维可视化精度低、喷灌需水量不明确及智能决策能力不足的问题，本文基于数字孪生六维架构（物理实体、虚拟模型、连接、服务、孪生数据与决策机制），提出一种孪生数据驱动的茶园三维可视化与系统设计方法。首先，基于 OPC UA 构建双向数据通道，结合 MySQL 集成多源传感器数据，为虚拟模型提供实时孪生数据支持。其次，基于孪生数据在 3ds Max 中进行茶树参数化建模，融合粒子系统、动态着色器、环境光遮蔽（AO）与多细节层次（LOD）技术，实现虚拟茶园的动态三维可视化。最后，集成 FAO Penman-Monteith 公式、AquaCrop 模型与长短期记忆网络（LSTM），构建 AquaCrop-LSTM 需水量预测模型，并在 Unity 中封装形成"感知-映射-决策-反馈"闭环系统。实验表明：LOD 使帧率提升 121%，顶点数减少 93.7%；AquaCrop-LSTM 模型的平均绝对误差为 0.251 mm，决定系数 R^2=0.927，精度显著优于对比模型；系统在 30 并发用户压力测试下错误率低于 0.02%，响应稳定。该系统为茶园可视化监控与水资源高效管理提供了可靠技术支撑。

INTRODUCTION

As a globally significant economic crop, tea production requires precise management to achieve agricultural modernization. Digital twin technology, by constructing accurate mappings between physical entities and virtual environments, provides crucial support for agricultural digital transformation *(Mitsanis C et al., 2024)*. The theory of digital twins has evolved from the three-dimensional conceptual model proposed by *Grieves M et al. (2017)* to the five-dimensional structure introduced by *TAO F et al. (2019)*, which integrates service systems and data networks to enable physical–virtual collaboration.

In agriculture, digital twins have been applied to equipment, crops, and resource management. *Lang Y et al. (2025)* enhanced greenhouse harvesting performance through virtual–real path optimization. *Xu X. et al. (2025)* developed a growth twin platform for winter wheat. *Mirbod O. et al. (2025)* proposed a Sim2Real framework to improve strawberry detection in real environments.

Kim S. et al. (2024) supported single-plant lifecycle management of citrus; and *Alves et al. (2023)* optimized irrigation strategies using a meteorology–soil–crop response mechanism.

However, digital twin applications in complex open agricultural scenarios still face limitations in dimensionality and decision-making capability. To address high complexity, *Zhou C et al. (2022)* and *Wang H.J. et al. (2024)* introduced six-dimensional models incorporating visualization, learning, and decision-making, significantly enhancing system intelligence and interaction.

Existing tea garden digital twins mainly focus on state monitoring and information display, while showing weakness in predictive modeling and data-driven decision support. Therefore, this study targets an ecological tea garden in Rizhao and constructs a six-dimensional digital twin framework by introducing a "decision mechanism," forming a management loop of "data perception–dynamic mapping–decision execution–feedback optimization" to drive sprinkler irrigation and iteratively improve system performance.

MATERIALS AND METHODS

Six-Dimensional Digital Twin Model for Tea Gardens

Drawing on the orchard digital twin framework *(WANG H.J et al.,2024)*, this study constructs a six-dimensional digital twin architecture for tea gardens (Figure 1), integrating physical entity, virtual model, connection, service, twin data, and decision mechanism.

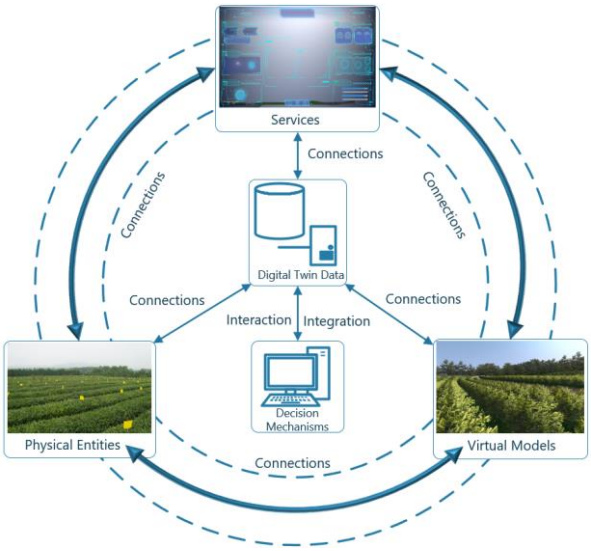

Fig. 1 - Tea Garden Digital Twin 6D Model

The model centers on a tight coupling between physical entities, virtual models, and twin data *(Liu X. et al., 2023)*. Twin data acts as the core nexus, aggregating real-time sensor and device information to drive dynamically evolving virtual models (*Mathur P. et al., 2024)*. The decision mechanism employs data fusion, threshold triggering, and time-series prediction to generate optimized strategies (e.g., for irrigation). Through a data feedback loop, it iteratively optimizes tea growth, equipment operation, and decisions. The service layer provides interactive interfaces such as environmental monitoring dashboards and weather simulation tools. The connection layer, enabled by bidirectional communication protocols, facilitates uplink (synchronizing physical states to the twin data platform) and downlink (transmitting control commands from the decision mechanism to physical terminals) interactions. This establishes a closed-loop management framework encompassing "data sensing-dynamic mapping-decision execution-feedback optimization," covering tea garden environmental perception, dynamic decision-making *(Wang J.J. et al., 2021)*, and full lifecycle management.

Overall Architecture of the Tea Garden Twin System

Based on the theoretical framework of the six-dimensional digital twin model, this study integrates key technology systems and management elements to construct the overall architecture of the tea garden digital twin system, as shown in Figure 2.

It is divided into the perception layer, data resource layer, model layer, application layer, and decision layer. Standardized interfaces enable bidirectional data flow and functional collaboration between layers, ultimately forming a closed-loop management mechanism *(Chen Y.P. et al., 2025)*.

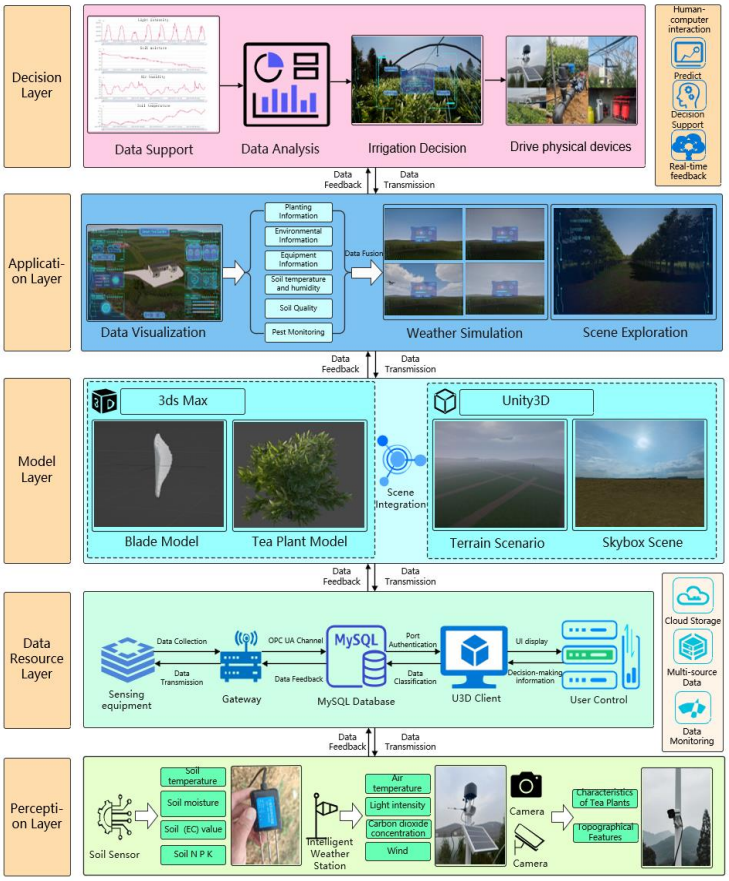

Fig. 2 - Architecture of the Digital Twin System for Tea Plantation Management

Tea Garden Environmental Perception

Environmental perception, as the “nerve endings” connecting the twin system with the physical world, enables real-time acquisition of tea garden environmental and growth conditions, supporting virtual modeling and data analysis. Soil sensors deployed at the surface, 5 cm, and 20 cm depths monitor temperature, moisture, electrical conductivity (EC), and nutrient information (N, P, K). A smart weather station records air temperature and humidity, light intensity, and CO_2 concentration, while imaging devices capture plant phenotypes and topographic features. These multi-source data provide essential inputs for constructing high-precision virtual tea garden models and enabling data-driven management.

Virtual Tea Garden Environment Construction

High-fidelity tea plant models form the foundation for 3D visualization. Based on multi-angle images of realistic leaf and branch morphology, parametric modeling was performed in 3ds Max. NURBS curves *(Kuraishi T. et al., 2025)* were used to create precise leaf meshes (Figure 3), while cylinder-based polygonal editing formed the branch structures.

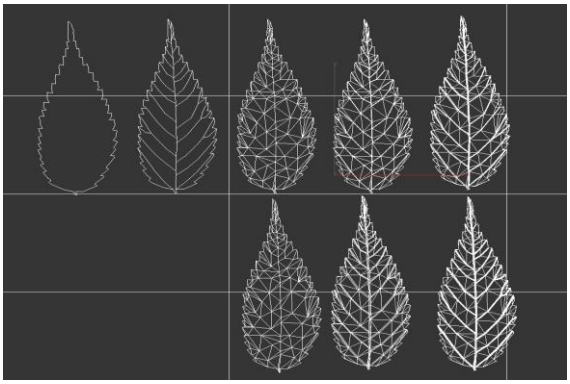

Fig. 3 - Leaf surface Mesh

High-resolution texture maps—Diffuse, Normal, and Displacement—were generated from images to represent surface color, roughness, and vein details. A skeletal system was built for branches, and leaves were assembled based on image features to produce a biologically accurate model.

In Unity3D, a digital twin of the tea plantation was constructed by integrating real-world data, including plants, meteorological and soil properties, and actual imagery, establishing a dual mapping between physical entities and digital models. Terrain textures were generated from image features using the Terrains system to form the geospatial environment.

Then, employ ambient occlusion (AO) *(Wu Y.T. et al., 2025)* to simulate the attenuation of ambient light caused by geometric occlusion, enhancing the realism of details in the virtual environment and assisting managers in spatial analysis of tea plant distribution. A tangent space-constrained hemispherical sampling domain was constructed based on normal vectors.

Uniformly distributed sample points were generated using the Hammersley low-discrepancy sequence $\{q_i'\}$. Its polar coordinates satisfy:

$$\emptyset_k = \frac{2\pi k}{N}, cos\theta_k = \sqrt{1-\xi_k} \tag{1}$$

Among these, $(\xi_k \in U[0,1))$ maps the sampling point to world space via the tangent space transformation matrix TBN, yielding the sampled position.

$$q_i = p_{world} + TBN \cdot (q_i' \cdot r) \tag{2}$$

Here, $r \in [0.1,2.0]$ represents the sampling radius, controlling the local occlusion range. After projecting the sampling point q_i into screen space, the theoretical depth $z_{q_i}$is computed and compared against the actual depth buffer value $d_{screen}(q_i)$ using a threshold to determine the visibility range.

$$V(q_i) = \begin{cases} 1, & d_{screen}(q_i) < z_{q_i} - \epsilon \\ 0, & otherwise \end{cases} \tag{3}$$

The anti-aliasing threshold $\epsilon = 0.05\ m$, is used to eliminate artifacts caused by deep buffer quantization errors.

The shielding coefficient calculation incorporates a distance attenuation function $w(d) = \max(0,1 - d/r)$ to suppress far-field interference. The normalized shielding strength is defined as:

$$AO(p) = 1 - \frac{1}{N}\sum_{i=1}^{N} V(q_i) \cdot w\left(||q_i - p_{world}||\right) \tag{4}$$

Finally, noise reduction is achieved using bilateral filtering that combines spatial and color domains:

$$AO_{final} = \frac{\sum_{j\in\Omega} AO(j) G_{\sigma_s}\left(||j-p||\right) G_{\sigma_r}\left(\Delta I_{jp}\right)}{\sum_{j\in\Omega} G_{\sigma_s}\left(||j-p||\right) G_{\sigma_r}\left(\Delta I_{jp}\right)} \tag{5}$$

Among these, G_σ represents the Gaussian kernel, $\sigma_s = 2.0$ denotes the spatial domain standard deviation (controlling the fuzzy range), and $\sigma_r = 0.2$ indicates the color domain standard deviation (controlling edge sensitivity).

As shown in Fig. 4(a)(d), the AO algorithm with normal alignment sampling and dynamic bilateral filtering enables virtual environment rendering to closely match the realism of the actual environment.

A particle system with Perlin noise was used to generate 3D cloud layers, producing controllable pseudo-random values to determine cloud particle distribution, density, and morphology. Precipitation simulation also adopted a particle system, with particle density and sound effects adjusted according to intensity levels from the twin data, enabling dynamic rain and snow effects, as shown in Fig. 4(b)(e).

Additionally, Unity's UGUI, Animation, and Timeline were combined to simulate environmental changes, allowing operators to adjust virtual parameters and observe tea plant responses. As shown in Fig. 4(c)(f), prolonged soil moisture below the threshold causes virtual leaves to yellow and curl, while adaptive decision prompts provide stress warnings and support irrigation optimization.

(a) Real Environment (b) Meteorological Simulation – Auto (c) Normal Leaf

(d) Virtual Environment (e) Meteorological Simulation – Manual (f) Yellowing & Curling Leaf

Fig. 4 - Comparative Analysis Between Virtual and Real Scenarios and Data-Driven Effects

Level of Detail (LOD) Processing

LOD technology balances rendering efficiency and visual quality in large-scale 3D environments. In tea garden models, dense vegetation with complex geometry can overload GPU vertex processing, reduce frame rates, and cause Moiré patterns, impacting both performance and accuracy.

(a)LOD_0 (b)LOD_1 (a)LOD_2 (b)LOD_3

Fig. 5 - Model Comparison Under Varied LOD Tiers

A four-level LOD model dynamically adjusts rendering quality by camera distance (Fig.5) *(Xia J.C. et al., 1997)*. Close range (0–15 m: LOD_0) uses high-detail models preserving fine textures and curves. Increasing distance activates lower-detail models (15–30 m: LOD_1; 30–60 m: LOD_2; >60 m: LOD_3), reducing polygon/vertex computations while maintaining visual coherence. Unity 2023 A/B testing (with/without LOD) yielded metrics in Table 1.

Table 1

Performance Evaluation of LOD Optimization

Metrics	Control Group	Experimental Group	Improvement Rate
Average Frame Rate (fps)	28.6	63.2	121.0%
Vertex Count (M)	171.5	10.8	93.7%
CPU Main Thread Time (ms)	17.4	7.7	55.7%
Rendering Thread Time (ms)	14.3	5.8	59.4%

Based on the quantitative analysis in Table 1, the four-level LOD technology demonstrated substantial rendering optimization within the tea garden visualization environment. The rendering thread time decreased by 59.4%, indicating a reduced CPU-to-GPU data transfer burden. The average frame rate increased to 63.2 FPS (+121.0%), stable performance under varying vegetation densities. Additionally, the vertex count was reduced by 93.7% (171.5M → 10.8M), which freed GPU bandwidth for advanced post-processing operations (e.g., SSGI) and improved overall visual fidelity.

Tea Plant Water Requirement Prediction Model

This study integrates the hydrological mechanisms of the AquaCrop model *(Alvar-Beltrán J. et al., 2025)* with an LSTM neural network, incorporating the FAO Penman-Monteith equation *(Shu Z. et al., 2025).*

Using air temperature, humidity, wind speed, light intensity, soil temperature, moisture, electrical conductivity, daily rainfall, and other meteorological indices as feature parameters, and water requirement as the target variable, an AquaCrop-LSTM prediction model was constructed. As shown in Table 2, the data were split into training and testing sets with a cutoff date of January 1, 2025. Monitoring timestamps were converted to UTC, missing values were handled using forward filling (max gap ≤ 4 hours), and discrete light intensity data were temporally integrated based on photon flux density theory.

$$R_s = \frac{\sum_{i=1}^{n}(lux_i \cdot \Delta t_i) \cdot 0.0079}{10^6} \quad (6)$$

In the equation, Δt_i represents the time difference (in seconds) between adjacent monitoring points. The conversion factor of 0.0079 is determined based on the photon energy conversion model, ultimately yielding the daily solar radiation amount (MJ/m²/day).

For parameters susceptible to transient disturbances, such as wind speed u_2 and soil EC values, outlier detection was performed using Tukey's fences method (IQR=1.5), with Winsorized truncation applied based on the 3σ principle. Z-score normalization was conducted separately for the feature matrix $X \in \mathbb{R}^{n \times m}$ and the target variable y:

$$z = \frac{x - \mu}{\sigma} \quad (7)$$

In particular, μ and σ are derived from the training set statistics to prevent information leakage.

Table 2

Source of Data

Stage	Period	Location	Data Volume (records)
Training Set	May 2022 – Dec 2022	Rizhao City, Shandong	6×10^3
	Jan 2023 – Dec 2023	Rizhao City, Shandong	8×10^3
	Jan 2024 – Dec 2024	Rizhao City, Shandong	1×10^4
Testing Set	Jan 2025 – Apr 2025	Rizhao City, Shandong	6×10^3

Reference evapotranspiration (ET_0) is calculated using the FAO Penman-Monteith equation, whose core formula is:

$$ET_0 = \frac{0.408\Delta(R_n - G) + \gamma \frac{900}{T + 273} u_2 (e_s - e_a)}{\Delta + \gamma(1 + 0.34u_2)} \quad (8)$$

In the formula: R_n—net radiation (MJ/m²/day)

Δ—slope of saturated vapor pressure-temperature curve (kPa/°C)

γ—dry-wet bulb constant (kPa/°C)

G—soil heat flux (MJ/m²/day)

u_2—wind speed (m/s)

e_s-e_a—saturated and actual vapor pressures, respectively

Tea plant water requirement is adjusted by crop coefficient (K_c) to modify ET_0:

$$ET_c = \max(K_c \cdot ET_0, 0) \quad (9)$$

To capture the lag effects and cyclical patterns of moisture demand, a multidimensional feature space is constructed by introducing a 7-day lag operator:

$$X_t^{(lag)} = [WaterReq_{t-1}, \ldots, Rainfall_{t-7}] \quad (10)$$

A total of 21-dimensional lag features were generated, covering the physiological delay cycle of tea plant water absorption.

During model training and evaluation, the Huber loss function (δ=0.5) was employed to balance mean squared error (MSE) and mean absolute error (MAE), enhancing robustness to outliers. Weight decay (weight_decay=1e⁻⁴) and gradient clipping (clip_grad_norm=0.5) were applied to constrain the parameter space, prevent overfitting, and stabilize the LSTM training process. The number of training epochs was set between 50 and 200, and batch sizes ranged from 32 to 128 to improve model generalization.

Twin Data-Driven Decision Control and Feedback Optimization

After obtaining physical data and constructing the virtual environment, the system uses real-time digital twin data to support virtual–physical interaction and intelligent decision-making, as shown in Fig.6.

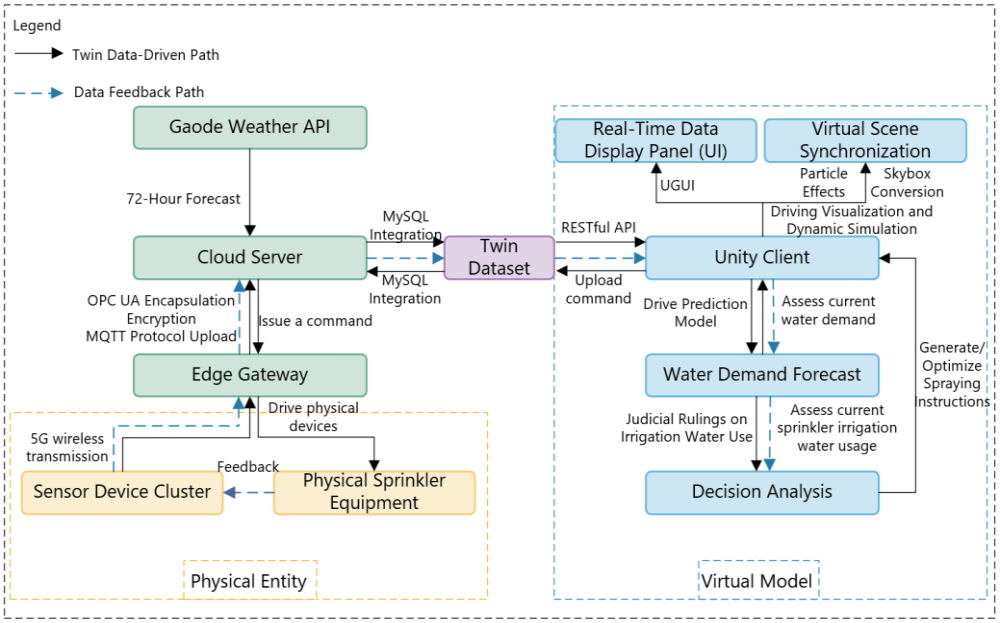

Fig. 6 - Data-Driven DT and Decision-Making Processes

Multi-source sensors collect environmental data, which is transmitted via 5G to an edge gateway and processed based on OPC UA (*Carballo J.A et al., 2024*), then forwarded to the cloud through MQTT. The cloud server uses MySQL to integrate the data into a dynamically updated digital twin dataset. The Unity client retrieves the data through a RESTful API, displays it in real time (Fig. 7(b)), and synchronizes the virtual environment, simulating lighting, weather, and crop growth through a particle system script.

At the smart decision level, the system combines digital twins with predictive models, uses control scripts and Unity coroutines for asynchronous control, analyzes data every 30 minutes, and based on the water demand predicted by the AquaCrop-LSTM model, calculates the actual irrigation amount Q using Equation (15) to generate precise control commands.

$$Q = \frac{10 \cdot ET_c \cdot A \cdot t}{\eta} \tag{11}$$

In the equation, A represents the sprinkler irrigation area (m²), t denotes the forecast period (day), and η indicates the sprinkler irrigation water utilization coefficient.

(a) Aerial View of Ecological Tea Garden *(b) Main Interface of Twin Tea Garden*

Fig. 7 - Tea Plantation Aerial View and Digital Twin Dashboard

(a) Physical Devices (b) Client Response Feedback

Fig. 8 - Tea Garden Physical Devices and Client Response

The control script analyzes state changes in the virtual model to generate irrigation commands, which are downlinked asynchronously via an edge gateway to precisely control physical irrigation equipment in the tea garden (as shown in Fig. 8(a)). The resulting environmental parameters then drive synchronous updates in the virtual environment (see Fig. 8(b)).

These state data are fed back into the decision-making mechanism and integrated with the digital twin dataset to optimize decisions, effectively preventing water stress and disease spread caused by under- or over-irrigation. This enables closed-loop precision irrigation control.

RESULTS

Prediction Model Validation

To evaluate the performance of the AquaCrop-LSTM model, it was compared against three other models—LightGBM, TCN-Transformer, and Random Forest—using MAE, MSE, and R² under consistent input features and hyperparameter optimization. AquaCrop-LSTM outperformed all others in every metric.

As shown in Figure 9, the model demonstrated high accuracy in predicting tea plant water demand, with absolute errors below 0.4 mm in 94.5% of cases. Its MAE (0.251 mm) was 19.7% lower than that of LightGBM, the second-best model, due to its effective integration of crop growth modeling and temporal feature extraction via LSTM. During the high-demand period (March 15–25, 2025), the average deviation was 0.12 mm, and its MSE (0.166 mm²) was 34.0% lower than TCN-Transformer (0.251 mm²).

Table 3

Comparison of Model Performance

Models	MAE/(mm)	MSE/(mm)	R^2
LightGBM	0.314	0.219	0.904
TCN-Transformer	0.344	0.251	0.878
Random Forest	0.433	0.302	0.852
AquaCrop-LSTM	**0.251**	**0.166**	**0.927**

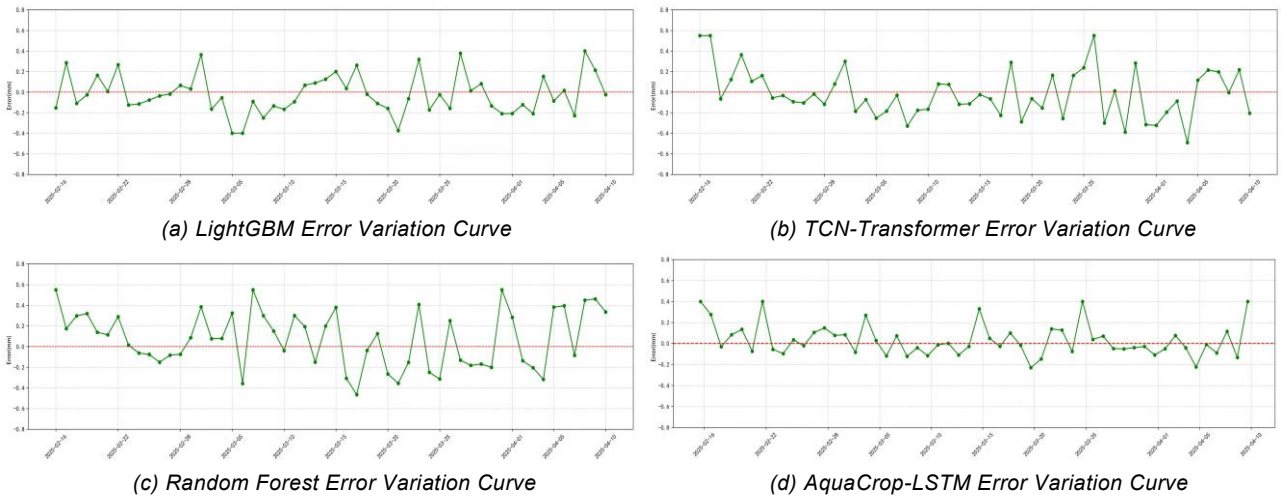

(a) LightGBM Error Variation Curve (b) TCN-Transformer Error Variation Curve

(c) Random Forest Error Variation Curve (d) AquaCrop-LSTM Error Variation Curve

Fig. 9 - Comparison of Error for Each Model Folded Line

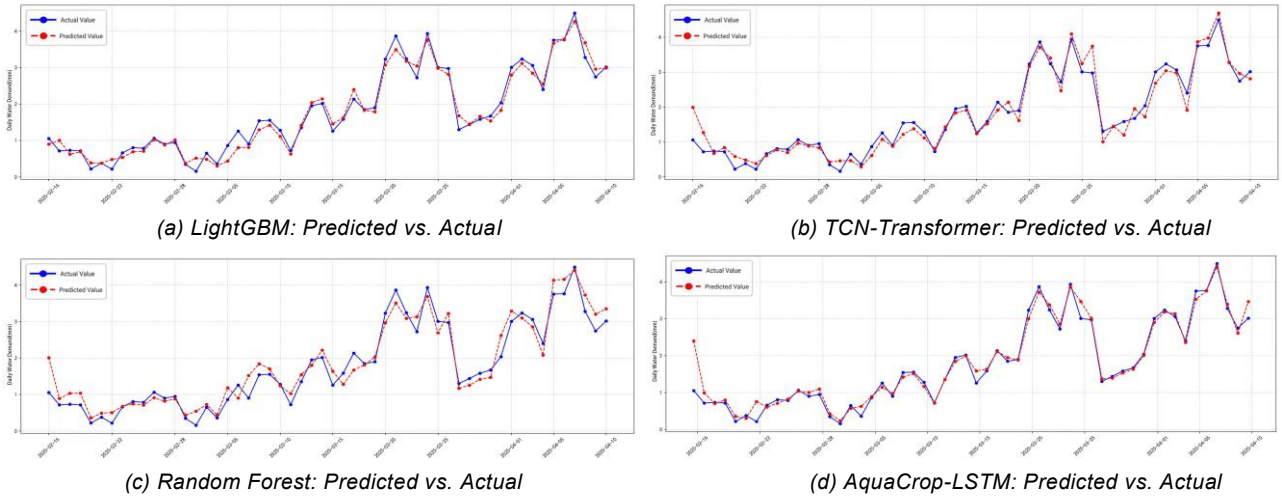

(a) LightGBM: Predicted vs. Actual

(b) TCN-Transformer: Predicted vs. Actual

(c) Random Forest: Predicted vs. Actual

(d) AquaCrop-LSTM: Predicted vs. Actual

Fig. 10 - Comparison of Predicted and True Values for Each Model Folded Line

Under extreme weather conditions, prediction errors reached 32.6% and 28.4% on February 16 (frost) and April 10 (heavy rainfall), respectively, due to input deviations from abrupt environmental changes (Fig. 10). In contrast, TCN-Transformer showed significant lag errors during high water-demand periods (March 20–April 1), while AquaCrop-LSTM effectively integrated environmental factors—including soil temperature, moisture, light, and rainfall—via multi-scale feature fusion, enhancing timeliness and robustness under sudden weather shifts.

In summary, by combining hydrological mechanisms of crop modeling with data-driven methods, the AquaCrop-LSTM model outperforms comparative models in both prediction accuracy and stability. It achieved a 38.1% reduction in error standard deviation and a 2.3% improvement in R^2 in high-value intervals, providing a reliable theoretical basis for precision irrigation management in tea gardens.

Twin System Stability Validation

To evaluate the stability of the tea garden digital twin system under multi-user and high-volume data transmission, gradient stress testing was conducted in Unity 2023.1.1f1c1. Seven concurrency levels (1 to 30) were set, each running 360 cycles processing 364,000 multi-source heterogeneous data per cycle. Performance was sampled every 200ms, focusing on CPU usage, memory consumption, response time, and transmission error rate, with thresholds given in Table 4.

Table 4

Performance Metric Thresholds for Stress Testing

Concurrency Level	Response time (ms)	Memory usage (MB)	CPU usage (%)	Average Error Rate (%)
1	≤800	≤500	≤30	≤0.01
5	≤1200	≤800	≤40	≤0.01
10	≤1800	≤1200	≤50	≤0.015
15	≤2500	≤1500	≤60	≤0.015
20	≤3500	≤1800	≤70	≤0.02
25	≤4500	≤2000	≤80	≤0.02
30	≤6000	≤2200	≤90	≤0.025

As shown in Figure 11, as concurrency increased from 1 to 30, CPU usage rose from 20–25% to 80–85%, stabilizing at 84%±2%; memory usage grew from 400–500 MB to 1900–2100 MB, and response time extended from 500–600 ms to 4800–5100 ms—all within acceptable thresholds (CPU <90%, response time <6000 ms). The transmission error rate remained below 0.02%. Dynamic thread scheduling effectively prevented resource contention, with no memory leaks or abnormal delays.

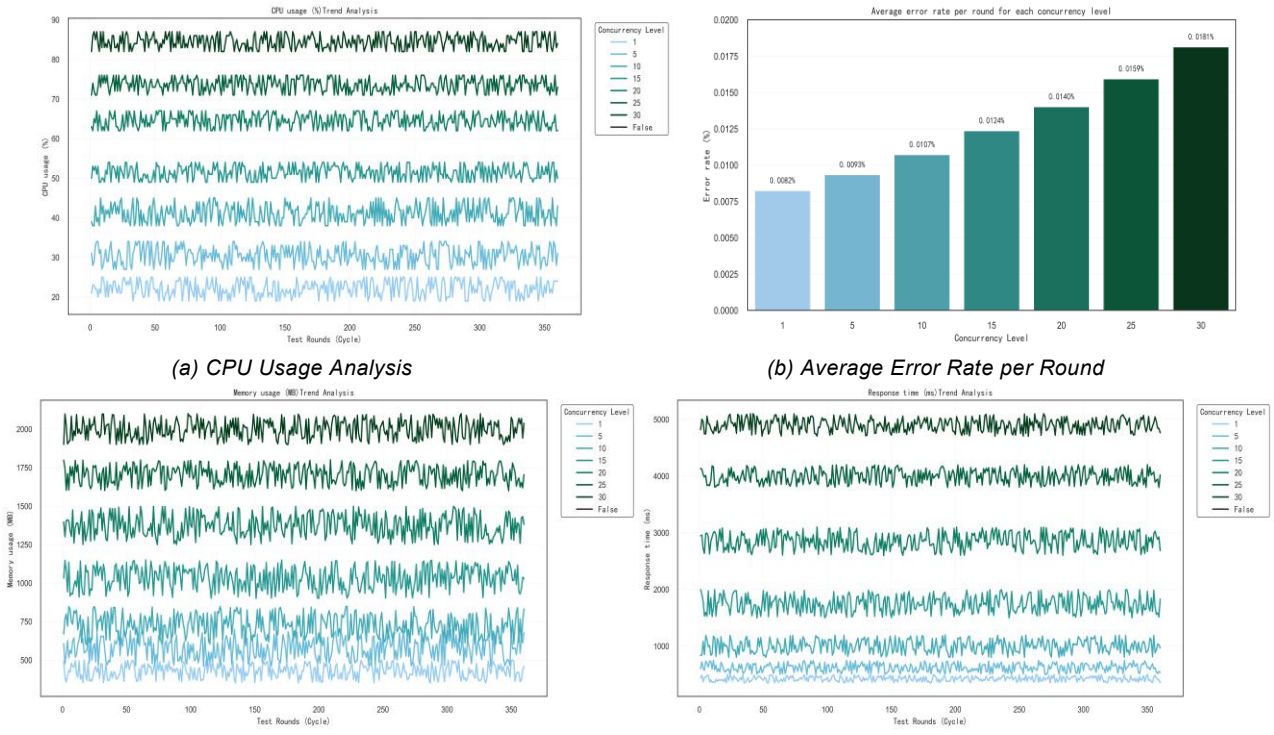

(a) CPU Usage Analysis *(b) Average Error Rate per Round*

(c) Memory Usage Analysis *(d) Response Time*

Fig. 11 - Trend Chart of Performance Metrics Across Concurrency Levels

In conclusion, the system maintains a very low error rate (<0.02%) under high concurrency (30 users) and large data throughput (364,000 entries/cycle), effectively mitigating resource contention and balancing load to ensure reliability and stability in complex agricultural digital twin applications.

CONCLUSIONS

This study integrates OPC UA and MySQL for multi-source data connectivity, together with high-precision parametric models built in 3ds Max and Unity, enhanced through particle systems, dynamic shaders, ambient occlusion (AO), and LOD techniques. Combined with a hybrid water-demand prediction model that incorporates the FAO Penman–Monteith equation, AquaCrop mechanisms, and LSTM networks, a six-dimensional digital twin system for tea garden management was developed, enabling continuous sensing, virtual–physical mapping, data-driven prediction, and closed-loop control. The system provides high-fidelity real-time visualization of tea plants and their environment, and the AquaCrop–LSTM model achieves superior performance (MAE = 0.251 mm, R^2 = 0.927). Under 30 concurrent users and 364,000 data records per cycle, the platform maintained stable CPU usage (84% ± 2%) with an error rate below 0.02%, demonstrating strong robustness and scalability. Overall, the proposed framework offers reliable technical support for visual monitoring, irrigation optimization, and intelligent decision-making in tea gardens, and provides a transferable reference for precision irrigation in other perennial crops.

ACKNOWLEDGEMENT

This research was supported by the following projects: Shandong Provincial Science and Technology Achievement Transfer and Transformation Subsidy Project (Shandong-Chongqing Science and Technology Collaboration) (2021LYXZ019) and the Taishan Industrial Leading Talent Project.

REFERENCES

[1] Alvar-Beltrán J., Setti A., Mugo J., Bucor N., Bejenaru G., Gialletti A., Druta A. (2025). Assessing climate change impacts and adaptation strategies for key crops in the Republic of Moldova using the AquaCrop model [J]. *European Journal of Agronomy*, 164: 127530.

[2] Alves R.G., Maia R.F., Lima F. (2023). Development of a Digital Twin for smart farming: Irrigation management system for water saving[J]. *Journal of Cleaner Production*, 388:135920.

[3] Carballo J.A., Bonilla J., Fernández-Reche J., Antonio Luis Avila Marin., Díaz B. (2024). Modern SCADA for CSP Systems Based on OPC UA, Wi-Fi Mesh Networks, and Open-Source Software[J]. *Energies*, 17(24): 6284.

[4] Chen Y.P., Karkaria V., Tsai Y.K., Rolark F., Quispe D., Gao R.X., Cao J., Chen W. (2025). Real-time decision-making for digital twin in additive manufacturing with model predictive control using time-series deep neural networks [J]. *arXiv preprint arXiv:2501.07601*.
[5] Grieves M., Vickers J. (2017). Digital twin: Mitigating unpredictable, undesirable emergent behavior in complex systems[J]. *Transdisciplinary perspectives on complex systems: New findings and approaches*, 85-113.
[6] Kim S., Heo S. (2024). An agricultural digital twin for mandarins demonstrates the potential for individualized agriculture [J]. *Nature Communications*, 15(1): 1561.
[7] Kuraishi T., Takizawa K., Tezduyar T.E. (2025). A general-purpose IGA mesh generation method: NURBS Surface-to-Volume Guided Mesh Generation [J]. *Computational Mechanics*, 75(1): 159-169.
[8] Lang Y., Zhang Y., Sun T., Chai X., Zhang N. (2025). Digital twin-driven system for efficient tomato harvesting in greenhouses [J]. *Computers and Electronics in Agriculture*, 236: 110451.
[9] Xin L., Jiang D., Bo T., Feng X., Guozhang J., Ying S., Jianyi K., Gongfa L. (2023). A systematic review of digital twin about physical entities, virtual models, twin data, and applications [J]. *Advanced Engineering Informatics*, 55: 101876.
[10] Mathur P., Sharma C., Azeemuddin S. (2024). Autonomous inspection of high-rise buildings for façade detection and 3D modeling using UAVs [J]. *IEEE Access*, 12: 18251-18258.
[11] Mirbod O., Choi D., Schueller J.K. (2025). From Simulation to Field Validation: A Digital Twin-Driven Sim2real Transfer Approach for Strawberry Fruit Detection and Sizing[J]. *AgriEngineering*, 7(3): 81.
[12] Mitsanis C., Hurst W., Tekinerdogan B. (2024). A 3D functional plant modelling framework for agricultural digital twins [J]. *Computers and Electronics in Agriculture*, 218: 108733.
[13] Shu Z., Jin J., Menzel L., Zhang J., Luo J., Wang G., Cui W., Guan T., Liu Y. (2025). Evaluating the effectiveness of different surface resistance schemes coupled with Penman-Monteith model for estimating actual evapotranspiration − A global comparative study [J]. *Journal of Hydrology*, 656: 133047.
[14] Tao F. (2019). Five-dimensional digital twin model and its ten applications [J]. *Computer Integrated Manufacturing Systems*, 25(1): 1.
[15] Wang H.J., Lin J.Q., Zou X.J., Zhang P., Zhou M.X., Zou W.R., Tang Y.C., Luo L.F. (2024). Construction of orchard virtual interaction system based on digital twin (基于数字孪生的果园虚拟交互系统构建) [J]. *Journal of System Simulation*, 36(6): 1493.
[16] Wang J.J., Wang S.H., Zhang L.B., Zhang Z. (2021). Intelligent risk decision system for compressor station equipment based on digital twin (基于数字孪生的压气站场设备风险智能决策系统) [J]. *Natural Gas Industry*, 41(7).
[17] Wu Y.T. (2025). Efficient Stereo-Aware Screen-Space Ambient Occlusion with Adaptive Computation[J]. *IEEE Computer Graphics and Applications*.
[18] Xia J.C., El-Sana J., Varshney A. (1997). Adaptive real-time level-of-detail based rendering for polygonal models[J]. IEEE Transactions on Visualization and Computer graphics, 3(2): 171-183.
[19] Xu X., Gao F., Xiong D., Fan Z., Xiong S., Dong P., Qiao H., Ma X. (2025). Digital twin-based winter wheat growth simulation and optimization[J]. Field Crops Research, 329: 109953.
[20] Zhou C., Sun K. T., Li J., Yu C.G., Kai J. (2022). Workshop 3D visual monitoring system based on digital twin [J]. *Computer Integrated Manufacturing Systems*, 28(3): 758.